DYNAMIC STEADY ANTIPLANE SHEAR CRACK GROWTH IN AN ELASTIC-PLASTIC MATERIAL

A. S. Douglas*, L. B. Freund* and D. M. Parks**

*Division of Engineering, Brown University, Providence, RI 02912, USA
**Department of Mechanical Engineering, Massachusetts Institute of Technology, Cambridge, MA 02139, USA

ABSTRACT

A numerical analysis of steady-state crack growth in an elastic-ideally plastic material under small scale yielding conditions is presented. Crack growth is in the antiplane shear mode and inertial resistance of the material to motion is included. The numerical procedure is based on the finite element method. It is found that, with increasing crack tip speed, the active plastic zone becomes smaller and less concentrated in the direction of growth, the crack opening angle remains unchanged, and the crack tip strain singularity becomes weaker.

KEY WORDS

Fracture mechanics; elastic-plastic fracture; dynamic fracture; computational mechanics; finite element method.

INTRODUCTION

The purpose of this paper is to report on a study concerned with the influence of inertia on the deformation field near the tip of an extending crack in an elastic-ideally plastic solid. The particular problem under consideration is the steady-state growth of a crack in the antiplane shear mode through a body of elastic-plastic, nonstrain-hardening material under small scale yielding conditions. Inertial resistance of the material to motion is included explicitly. For this situation, the deformation is time-independent as viewed by an observer fixed at the tip of the semi-infinite crack in an otherwise unbounded body. According to the small scale yielding hypothesis, the elastic-plastic field in the crack tip region is controlled by the surrounding elastic field. A useful measure of this surrounding field, for any given crack tip speed v, is the linear elastic stress intensity factor k, which is assumed to be known in terms of body geometry and applied loads from solution of a suitable elastic crack problem.

This same problem, but with inertial effects neglected, was studied in some detail by Rice (1968) and Chitaley and McClintock (1971). Each employed incremental plastic stress-strain relations based on the associated flow rule and a yield condition suitable for the antiplane deformation mode in a nonhardening material. For this case, both the Tresca and Mises criteria reduce to

$$\sigma_{13}^2 + \sigma_{23}^2 = \tau_o^2 \tag{1}$$

where σ_{13} and σ_{23} are the operative shear stress components and τ_o is the flow stress in pure shear. They showed that the principal shear lines in the active plastic zone are straight, and Rice (1968) determined the distribution of plastic strain on the line directly ahead of the tip in terms of the unknown distance between the tip and the elasticplastic boundary. Chitaley and McClintock (1971) went on to numerically integrate the field equations. In a more recent study of the same problem, Dean and Hutchinson (1979) noted some discrepancies between the results of their finite-element calcualtions and the numerical results of Chitaley and McClintock. Whereas the latter authors assumed that the principal shear lines in the active plastic zone were all members of a centered fan, the results of Dean and Hutchinson suggest that, in a portion of the active plastic zone, the shear lines do not form a centered fan. Results of other studies on quasi-static steady antiplane shear crack growth have recently been reported by Anderson (1974), Amazigo and Hutchinson (1978) and Sorenson (1978).

If material inertia is taken into account in this steady-state problem, then the system of governing equations retains the property of hyperbolicity in the active plastic zone. However, the directions of principal shear lines are no longer characteristic directions. Instead, there exist two families of characteristic curves which coalesce to a single family in the limit as crack speed $v \to 0$. No clear picture of the structure of the characteristic net within the active plastic zone is yet available. Attempts at extracting the asymptotic behavior of the crack tip field for points arbitrarily close to the crack tip have been made by Slepyan (1976) and by Achenbach, Burgers, and Dunayevsky (1979). Some results have been derived, but they have the unfortunate feature that the deformation fields do not reduce to the correct near tip field (cf. Chitaley and McClintock, 1971) as crack speed $v \to 0$. It is likely that the extent of the region in which the asymptotic results are valid also vanishes as $v \to 0$. Results of another study on steady-state dynamic antiplane shear crack growth have been reported by Achenbach and Kanninen (1978).

In the following two sections, a numerical analysis based on the finite element method is described. In the next section the governing equations are put in suitable form, and the numerical procedure is described in the following section. Some general conclusions are drawn in the final section.

FORMULATION

In the development which follows, all variables are referred to a translating set of Cartesian coordinates (x_1, x_2, x_3) in the body. The x_3-axis coincides with the edge of the crack and the crack edge (or tip) moves in the x_1-direction with speed v; see Fig. 1. It is assumed that the crack has grown for some time under the action of slowly varying remote loading, characterized by the elastic stress intensity factor k. A long-time, or steady state, solution is then sought under the assumption that such a steady state solution will indeed be achieved after all transients associated with initiation have died out.

The displacement vector is in the x_3-direction and its magnitude u_3 depends only on position in the x_1, x_2-plane. It is convenient to introduce the following nondimensional coordinates and corresponding field quantities:

$$x = x_1 \tau_o^2/k^2 \qquad y = x_2 \alpha \tau_o^2/k^2 \qquad w = \mu \tau_o u_3/k^2 \tag{2}$$

$$\gamma_x = 2\mu\varepsilon_{31}/\tau_o \qquad \gamma_y = 2\mu\varepsilon_{32}/\tau_o \tag{3}$$

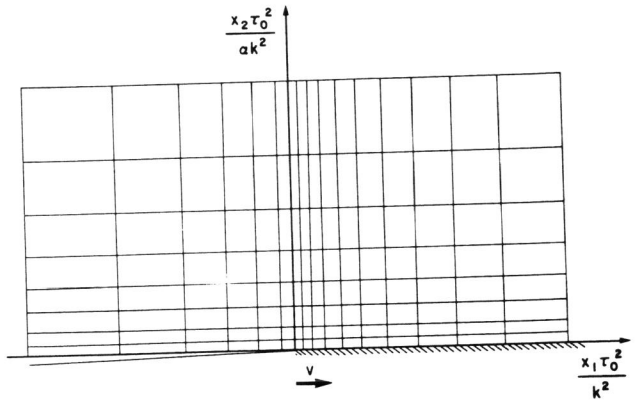

Fig. 1. The plane of deformation, showing a coarse representation of the finite element mesh.

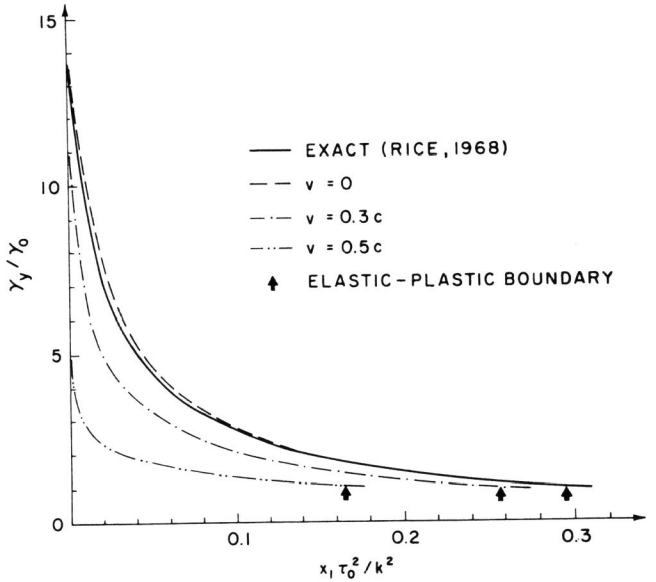

Fig. 2. The y-component of total shear strain vs. distance ahead of the moving crack tip, showing a comparison of numerical and theoretical results.

$$\tau_x = \sigma_{31}/\tau_o \qquad \tau_y = \sigma_{32}/\tau_o \tag{4}$$

where μ is the elastic shear modulus, ε_{31} and ε_{32} are components of the infinitesimal strain tensor, $\alpha = \sqrt{1-v^2/c^2}$ and c is the elastic wave speed $\sqrt{\mu/\rho}$, where ρ is material mass density.

Because fields are steady as seen by an observer moving in the x_1-direction at speed v, time differentiation is equivalent to the operation $-v\partial(\ )/\partial x_1$. In the absence of body forces, the equation of motion then has the form

$$\tau_{x,x} + \alpha\tau_{y,y} = (v/c)^2\, w_{,xx} \tag{5}$$

where the standard comma notation for partial differentiation is employed. The total strain is decomposed additively into elastic and plastic portions,

$$\gamma_\beta = \gamma_\beta^e + \gamma_\beta^p \ , \qquad \beta = x \text{ or } y \tag{6}$$

and the elastic strain is related to the stress according to

$$\tau_\beta = \gamma_\beta^e = (\gamma_\beta - \gamma_\beta^p) \ . \tag{7}$$

By making use of the strain-displacement relations

$$\gamma_x = w_{,x} \quad \text{and} \quad \gamma_y = \alpha w_{,y} \tag{8}$$

along with (7), the equation of motion (5) may be written in the form

$$w_{,xx} + w_{,yy} = \alpha^{-2}\gamma^p_{x,x} + \alpha^{-1}\gamma^p_{y,y} \tag{9}$$

The asymptotic behavior of the stress components as $r = \sqrt{x^2 + y^2} \to \infty$ is chosen to be consistent with the small scale yielding hypothesis. Thus, in nondimensional form, the stress components are required to approach the values

$$\tau_x \to -\frac{\sin(\theta/2)}{\alpha\sqrt{2\pi r}} \ , \qquad \tau_y \to \frac{\cos(\theta/2)}{\sqrt{2\pi r}} \tag{10}$$

where $\theta = \arctan(y/x)$, as $r \to \infty$.

NUMERICAL PROCEDURE

To serve as a basis for developing a numerical procedure, the governing field equation (9) is converted to the variational form

$$\int_A \nabla w^* \cdot \nabla w \, dA = -\int_A w^*(\alpha^{-2}\gamma^p_{x,x} + \alpha^{-1}\gamma^p_{y,y})dA + \int_{\partial A} w^*(n \cdot \nabla w)dS \tag{11}$$

where A is any region of the plane bounded by ∂A, ∇ is the two-dimensional gradient operator, n is the unit normal to ∂A pointing out of A, and w^* is an arbitrary function having the same smoothness properties and satisfying the same kinematic constraints as w. The region $y > 0$ is then divided into finite elements, and the displacement is approximated by $w = \phi_i\delta_i$, $i = 1,\ldots n$ and summation implied, where δ_i are the values of the displacement at n points, or nodes, and ϕ_i are the interpolation functions. Likewise, $w^* = \phi_i\delta_i^*$. The $n \times n$ stiffness matrix for any region A is then

$$K_{ij} = \int_A \nabla\phi_i \cdot \nabla\phi_j \, dA \tag{12}$$

Consider now the rectangular area shown in Fig. 1. After integration by parts of the area integral, the right side of (11) becomes $R_i\delta_i^*$ where

$$R_i = \int_A [\alpha^{-2}\gamma^p_x \phi_{i,x} + \alpha^{-1}\gamma^p_y \phi_{i,y}] \, dA \tag{13}$$

$$+ \int_{\Gamma_1} \phi_i(2\pi r)^{-1/2}[n_y \cos(\theta/2) - \alpha^{-1} n_x \sin(\theta/2)] \, dS + \int_{\Gamma_2} \phi_i[-\tau_x + (v/\alpha c)^2\gamma^p_x]dy.$$

The path Γ_1 is the perimeter of the rectangular region in Fig. 1, except for the portion of the left boundary in the wake region which is identified as Γ_2. It is clear from (13) that boundary tractions are imposed on Γ_1 which are consistent with the asymptotic stresses (10). For this to be a reasonable identification, points on Γ_1 should be far from the crack tip compared to the plastic zone size.

Thus, with the finite element approximation and with δ_i^* arbitrary, the variational statement of the governing equations (11) may be reduced to the system of linear equations

$$K_{ij}\,\delta_j = R_i(\gamma^p_x, \gamma^p_y, \text{ known quantities}) \tag{14}$$

In order to solve these equations for the displacements δ_i, the plastic strains must be known. These are unknown a priori, however, and an iterative procedure is adopted. Before describing the procedure, it is necessary to elaborate on the stress-strain relation. Following Dean and Hutchinson, the present analysis proceeds with a material which exhibits isotropic hardening and bilinear response in uniaxial, monotonic shearing. In nondimensional form, the stress-strain relations are

$$\begin{aligned} \dot\gamma_\beta &= \dot\tau_\beta \qquad , \ \tau < 1 \\ G\dot\gamma_\beta &= G\dot\tau_\beta + (1-G)\,\tau_\beta\dot\tau/\tau \ , \ \tau \geq 1 \end{aligned} \tag{15}$$

where $\beta = x$ or y, $\tau = \sqrt{\tau_x^2 + \tau_y^2}$ and G is the ratio of the plastic tangent modulus to the elastic modulus μ . The method of Rice and Tracey (1971) is adopted for computing the stress field from a given strain field for any specified value of the hardening parameter. The steps in the numerical procedure may be summarized as follows:

1. Assume elastic behavior, i.e., $G = 1$, and calculate the elastic displacements at the nodes. This is the first estimate, say $\delta_j(1)$.

2. Decrease the value of G by a small amount.

3. Calculate the total strains $\gamma_\beta(i)$ from the ith estimate of displacement $\delta_j(i)$ by means of the strain-displacement relation.

4. Apply the method of Rice and Tracey (1971) to calculate the stresses $\tau_\beta(i)$ from the stress-strain relations.

5. Determine the plastic strain $\gamma_\beta P(i)$ according to (7).

6. Calculate the $(i+1)$th estimate of displacement $\delta_j(i+1)$ from (13).

7. Compare $\delta_j(i+1)$ to $\delta_j(i)$. If the difference is sufficiently small, go to step 8; otherwise, increment the index i by 1 and return to step 3.

8. If $G = 0$, the process is complete; otherwise, reset $i = 1$ and return to step 2.

The finite element calculations were based on an array of 1800 rectangular elements, each comprising four constant strain triangles. The size of the smallest element was approximately 0.3% of the maximum extent of the plastic zone. Within each cycle in the iteration, stresses were computed by integrating incrementally in the negative x-direction from the right hand boundary along lines of constant y. For a repeated substitution procedure of the type employed here convergence is essentially linear, and typically 30 to 100 cycles were required to meet the convergence criterion set in step 7, i.e., that the square root of the sum of the squares of the nodal displacement differences is less than 0.0001.

RESULTS

The numerical scheme was first applied for the special case of quasi-static crack growth, i.e., for $v = 0$, so that the computed strain distribution on the prospective fracture plane could be compared to the exact result given by Rice (1968). As can be seen from Fig. 2, the computed strain distribution is very close to the exact distribution everywhere except in the elements nearest the crack tip where the numerical scheme cannot reproduce the logarithm squared singularity in the exact result. The calculated active plastic zone for quasi-static growth is shown in Fig. 3, along with the familiar circular plastic zone for the stationary crack under monotonic loading up to the same k level in the same material. The shape of the active plastic zone is quite similar to the shape computed by Dean and Hutchinson (1979), but the extent in the x-direction is found here to be roughly 20% smaller. The principal shear direction at any point within 20° of the x-axis was found to be nearly radial, except within elements very near to the crack tip. Finally, a small region of reversed plastic flow was observed in the wake region along the crack faces.

The numerical procedure was then applied for crack growth speeds equal to 30% and 50% of the elastic shear wave speed c. As shown in Fig. 3, it was found that the active plastic zone became smaller and less concentrated in the crack growth direction with increasing crack tip speed (at a given level of remote k). The level of strain on $y = 0$ at a given value of $x_1/(k/\tau_o)^2$ also decreases with increasing speed, as shown in Fig. 2. Local behavior is consistent with the result that γ_y is proportional to $(\ell n\, x)^2$ near the tip for $v = 0$ (Rice, 1968), but is proportional to $\ell n\, x$ near the tip for $v > 0$ (Slepyan, 1976). The crack opening profile is shown in Fig. 4 for the three speeds $v = 0$, $0.3c$, $0.5c$. If the crack opening angle is chosen to be the slope of the opening profile at some distance behind the tip equal to a small fraction of the active plastic zone size (extent along $y = 0$) for quasi-static growth, say $0.05(k/\tau_o)^2$, then it appears that the crack opening angle is insensitive to variations in crack speed. On the other hand, in order to maintain a specific level of strain at a fixed distance ahead of the tip for $v > 0$, as well as for $v = 0$, it is necessary for $k(v > 0)$ to be substantially larger than the corresponding $k(v = 0)$. This is indeed the case for running fractures in materials which do not exhibit a strain rate induced mechanism change during fast fracture.

The geometry of the principal shear lines in the active plastic zone is unknown at present so that no comparison with exact results is possible. However, on the basis of these calculations it appears that the principal shear lines may differ significantly from radial lines during rapid crack growth.

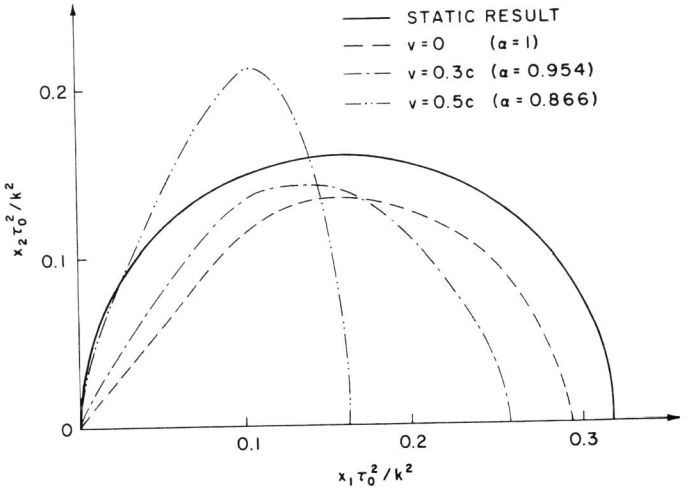

Fig. 3. The boundary of the primary active plastic zone for quasi-static crack growth and dynamic growth at two different speeds.

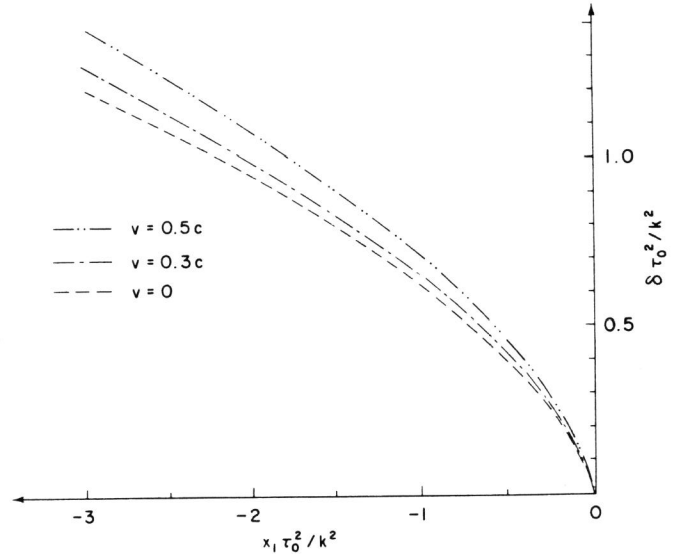

Fig. 4. Crack face opening displacement vs. distance behind the moving crack tip.

ACKNOWLEDGEMENT

The research support of the National Science Foundation, Solid Mechanics Program, through grants ENG77-15564 to Brown University and ENG77-06475 to Yale University, is gratefully acknowledged.

REFERENCES

Achenbach, J. D., P. Burgers and V. Dunayevsky (1979). Near tip plastic deformations in dynamic fracture problems. In N. Perrone and S. Atluri (Eds.), Nonlinear and Dynamic Fracture Mechanics, AMD-Vol. 35, American Society of Mechanical Engineers, New York, pp. 105-124.

Achenbach, J. D. and M. F. Kanninen (1978). Crack tip plasticity in dynamic fracture mechanics. In N. Perrone, H. Liebowitz, D. Mulville and W. Pilkey (Eds.), Fracture Mechanics, The University of West Virginia Press. pp. 649-670.

Amazigo, J. C. and J. W. Hutchinson (1977). Crack tip fields in steady crack growth with linear strain hardening. J. Mech. Phys. Solids., 25, 81-97.

Anderson, H. (1974). Finite element treatment of a uniformly moving elastic-plastic crack tip. J. Mech. Phys. Solids, 22, pp. 285-308

Chitaley, A. D. and F. A. McClintock (1971). Elastic-plastic mechanics of steady crack growth under antiplane shear. J. Mech. Phys. Solids, 19, 147-163.

Dean, R. H. and J. W. Hutchinson (1979). Quasistatic steady crack growth in small scale yielding. Division of Applied Sciences Report MECH-11, Harvard University.

Rice, J. R. (1968). Mathematical analysis in the mechanics of fracture. In H. Liebowitz (Ed.), Fracture, Vol. II, Academic Press, New York, pp. 191-311.

Rice, J. R. and D. M. Tracey (1971). Computational fracture mechanics. In S. J. Fenves (Ed.), Numerical and Computer Methods in Structural Mechanics, Academic Press, New York, pp. 585-623.

Sorenson, E. P. (1978). A finite-element investigation of stable crack growth in antiplane strain. Int. J. Fracture, 14, pp. 485-500.